April 30, 2009
Preprint typeset using LaTeX style emulateapj v. 03/07/07

STACKED SEARCH FOR GRAVITATIONAL WAVES FROM THE 2006 SGR 1900+14 STORM

B. P. Abbott[17], R. Abbott[17], R. Adhikari[17], P. Ajith[2], B. Allen[2, 60], G. Allen[35], R. S. Amin[21], S. B. Anderson[17], W. G. Anderson[60], M. A. Arain[47], M. Araya[17], H. Armandula[17], P. Armor[60], Y. Aso[17], S. Aston[46], P. Aufmuth[16], C. Aulbert[2], S. Babak[1], P. Baker[24], S. Ballmer[17], C. Barker[18], D. Barker[18], B. Barr[48], P. Barriga[59], L. Barsotti[20], M. A. Barton[17], I. Bartos[10], R. Bassiri[48], M. Bastarrika[48], B. Behnke[1], M. Benacquista[42], J. Betzwieser[17], P. T. Beyersdorf[31], I. A. Bilenko[25], G. Billingsley[17], R. Biswas[60], E. Black[17], J. K. Blackburn[17], L. Blackburn[20], D. Blair[59], B. Bland[18], T. P. Bodiya[20], L. Bogue[19], R. Bork[17], V. Boschi[17], S. Bose[61], P. R. Brady[60], V. B. Braginsky[25], J. E. Brau[53], D. O. Bridges[19], M. Brinkmann[2], A. F. Brooks[17], D. A. Brown[36], A. Brummit[30], G. Brunet[20], A. Bullington[35], A. Buonanno[49], O. Burmeister[2], R. L. Byer[35], L. Cadonati[50], J. B. Camp[26], J. Cannizzo[26], K. C. Cannon[17], J. Cao[20], L. Cardenas[17], S. Caride[51], G. Castaldi[56], S. Caudill[21], M. Cavaglià[39], C. Cepeda[17], T. Chalermsongsak[17], E. Chalkley[48], P. Charlton[9], S. Chatterji[17], S. Chelkowski[46], Y. Chen[1, 6], N. Christensen[8], C. T. Y. Chung[38], D. Clark[35], J. Clark[7], J. H. Clayton[60], T. Cokelaer[7], C. N. Colacino[12], R. Conte[55], D. Cook[18], T. R. C. Corbitt[20], N. Cornish[24], D. Coward[59], D. C. Coyne[17], J. D. E. Creighton[60], T. D. Creighton[42], A. M. Cruise[46], R. M. Culter[46], A. Cumming[48], L. Cunningham[48], S. L. Danilishin[25], K. Danzmann[2, 16], B. Daudert[17], G. Davies[7], E. J. Daw[40], D. DeBra[35], J. Degallaix[2], V. Dergachev[51], S. Desai[37], R. DeSalvo[17], S. Dhurandhar[15], M. Díaz[42], A. Dietz[7], F. Donovan[20], K. L. Dooley[47], E. E. Doomes[34], R. W. P. Drever[5], J. Dueck[2], I. Duke[20], J. -C. Dumas[59], J. G. Dwyer[10], C. Echols[17], M. Edgar[48], A. Effler[18], P. Ehrens[17], E. Espinoza[17], T. Etzel[17], M. Evans[20], T. Evans[19], S. Fairhurst[7], Y. Faltas[47], Y. Fan[59], D. Fazi[17], H. Fehrmann[2], L. S. Finn[37], K. Flasch[60], S. Foley[20], C. Forrest[54], N. Fotopoulos[60], A. Franzen[16], M. Frede[2], M. Frei[41], Z. Frei[12], A. Freise[46], R. Frey[53], T. Fricke[19], P. Fritschel[20], V. V. Frolov[19], M. Fyffe[19], V. Galdi[56], J. A. Garofoli[36], I. Gholami[1], J. A. Giaime[19, 21], S. Giampanis[2], K. D. Giardina[19], K. Goda[20], E. Goetz[51], L. M. Goggin[60], G. González[21], M. L. Gorodetsky[25], S. Gossler[2], R. Gouaty[21], A. Grant[48], S. Gras[59], C. Gray[18], M. Gray[4], R. J. S. Greenhalgh[30], A. M. Gretarsson[11], F. Grimaldi[20], R. Grosso[42], H. Grote[2], S. Grunewald[1], M. Guenther[18], E. K. Gustafson[17], R. Gustafson[51], B. Hage[16], J. M. Hallam[46], D. Hammer[60], G. D. Hammond[48], C. Hanna[17], J. Hanson[19], J. Harms[52], G. M. Harry[20], I. W. Harry[7], E. D. Harstad[53], K. Haughian[48], K. Hayama[42], J. Heefner[17], I. S. Heng[48], A. Heptonstall[17], M. Hewitson[2], S. Hild[46], E. Hirose[36], D. Hoak[19], K. A. Hodge[17], K. Holt[19], D. J. Hosken[45], J. Hough[48], D. Hoyland[59], B. Hughey[20], S. H. Huttner[48], D. R. Ingram[18], T. Isogai[8], M. Ito[53], A. Ivanov[17], B. Johnson[18], W. W. Johnson[21], D. I. Jones[57], G. Jones[7], R. Jones[48], L. Ju[59], P. Kalmus[17], V. Kalogera[28], S. Kandhasamy[52], J. Kanner[49], D. Kasprzyk[46], E. Katsavounidis[20], K. Kawabe[18], S. Kawamura[27], F. Kawazoe[2], W. Kells[17], D. G. Keppel[17], A. Khalaidovski[2], F. Y. Khalili[25], R. Khan[10], E. Khazanov[14], P. King[17], J. S. Kissel[21], S. Klimenko[47], K. Kokeyama[27], V. Kondrashov[17], R. Kopparapu[37], S. Koranda[60], D. Kozak[17], B. Krishnan[1], R. Kumar[48], P. Kwee[16], P. K. Lam[4], M. Landry[18], B. Lantz[35], A. Lazzarini[17], H. Lei[42], M. Lei[17], N. Leindecker[35], I. Leonor[53], C. Li[6], H. Lin[47], P. E. Lindquist[17], T. B. Littenberg[24], N. A. Lockerbie[58], D. Lodhia[46], M. Longo[56], M. Lormand[19], P. Lu[35], M. Lubinski[18], A. Lucianetti[47], H. Lück[2, 16], B. Machenschalk[1], M. MacInnis[20], M. Mageswaran[17], K. Mailand[17], I. Mandel[28], V. Mandic[52], S. Márka[10], Z. Márka[10], A. Markosyan[35], J. Markowitz[20], E. Maros[17], I. W. Martin[48], R. M. Martin[47], J. N. Marx[17], K. Mason[20], F. Matichard[21], L. Matone[10], R. A. Matzner[41], N. Mavalvala[20], R. McCarthy[18], D. E. McClelland[4], S. C. McGuire[34], M. McHugh[23], G. McIntyre[17], D. J. A. McKechan[7], K. McKenzie[4], M. Mehmet[2], A. Melatos[38], A. C. Melissinos[54], D. F. Menéndez[37], G. Mendell[18], R. A. Mercer[60], S. Meshkov[17], C. Messenger[2], M. S. Meyer[19], J. Miller[48], J. Minelli[37], Y. Mino[6], V. P. Mitrofanov[25], G. Mitselmakher[47], R. Mittleman[20], O. Miyakawa[17], B. Moe[60], S. D. Mohanty[42], S. R. P. Mohapatra[50], G. Moreno[18], T. Morioka[27], K. Mors[2], K. Mossavi[2], C. MowLowry[4], G. Mueller[47], H. Müller-Ebhardt[2], D. Muhammad[19], S. Mukherjee[42], H. Mukhopadhyay[15], A. Mullavey[4], J. Munch[45], P. G. Murray[48], E. Myers[18], J. Myers[18], T. Nash[17], J. Nelson[48], G. Newton[48], A. Nishizawa[27], K. Numata[26], J. O'Dell[30], B. O'Reilly[19], R. O'Shaughnessy[37], E. Ochsner[49], G. H. Ogin[17], D. J. Ottaway[45], R. S. Ottens[47], H. Overmier[19], B. J. Owen[37], Y. Pan[49], C. Pankow[47], M. A. Papa[1, 60], V. Parameshwaraiah[18], P. Patel[17], M. Pedraza[17], S. Penn[13], A. Perraca[46], V. Pierro[56], I. M. Pinto[56], M. Pitkin[48], H. J. Pletsch[2], M. V. Plissi[48], F. Postiglione[55], M. Principe[56], R. Prix[2], L. Prokhorov[25], O. Punken[2], V. Quetschke[47], F. J. Raab[18], D. S. Rabeling[4], H. Radkins[18], P. Raffai[12], Z. Raics[10], N. Rainer[2], M. Rakhmanov[42], V. Raymond[28], C. M. Reed[18], T. Reed[22], H. Rehbein[2], S. Reid[48], D. H. Reitze[47], R. Riesen[19], K. Riles[51], B. Rivera[18], P. Roberts[3], N. A. Robertson[17, 48], C. Robinson[7], E. L. Robinson[1], S. Roddy[19], C. Röver[2], J. Rollins[10], J. D. Romano[42], J. H. Romie[19], S. Rowan[48], A. Rüdiger[2], P. Russell[17], K. Ryan[18], S. Sakata[27], L. Sancho de la Jordana[44], V. Sandberg[18], V. Sannibale[17], L. Santamaría[1], S. Saraf[32], P. Sarin[20], B. S. Sathyaprakash[7], S. Sato[27], M. Satterthwaite[4], P. R. Saulson[36], R. Savage[18], P. Savov[6], M. Scanlan[22], R. Schilling[2], R. Schnabel[2], R. Schofield[53], B. Schulz[2], B. F. Schutz[1, 7], P. Schwinberg[18], J. Scott[48], S. M. Scott[4], A. C. Searle[17], B. Sears[17], F. Seifert[2], D. Sellers[19], A. S. Sengupta[17], A. Sergeev[14], B. Shapiro[20], P. Shawhan[49], D. H. Shoemaker[20], A. Sibley[19], X. Siemens[60], D. Sigg[18], S. Sinha[35], A. M. Sintes[44], B. J. J. Slagmolen[4], J. Slutsky[21], J. R. Smith[36], M. R. Smith[17], N. D. Smith[20], K. Somiya[6], B. Sorazu[48], A. Stein[20], L. C. Stein[20], S. Steplewski[61], A. Stochino[17], R. Stone[42], K. A. Strain[48], S. Strigin[25], A. Stroeer[26], A. L. Stuver[19], T. Z. Summerscales[3], K. -X. Sun[35], M. Sung[21], P. J. Sutton[7], G. P. Szokoly[12], D. Talukder[61], L. Tang[42], D. B. Tanner[47], S. P. Tarabrin[25], J. R. Taylor[2], R. Taylor[17], J. Thacker[19], K. A. Thorne[19], K. S. Thorne[6], A. Thüring[16], K. V. Tokmakov[48], C. Torres[19], C. Torrie[17], G. Traylor[19], M. Trias[44], D. Ugolini[43], J. Ulmen[35], K. Urbanek[35], H. Vahlbruch[16], M. Vallisneri[6], C. Van Den Broeck[7], M. V. van der Sluys[28], A. A. van Veggel[48], S. Vass[17], R. Vaulin[60], A. Vecchio[46], J. Veitch[46], P. Veitch[45], C. Veltkamp[2], A. Villar[17], C. Vorvick[18], S. P. Vyachanin[25], S. J. Waldman[20], L. Wallace[17], R. L. Ward[17], A. Weidner[2], M. Weinert[2], A. J. Weinstein[17], R. Weiss[20], L. Wen[6, 59], S. Wen[21], K. Wette[4], J. T. Whelan[1, 29],

S. E. Whitcomb[17], B. F. Whiting[47], C. Wilkinson[18], P. A. Willems[17], H. R. Williams[37], L. Williams[47], B. Willke[2, 16], I. Wilmut[30], L. Winkelmann[2], W. Winkler[2], C. C. Wipf[20], A. G. Wiseman[60], G. Woan[48], R. Wooley[19], J. Worden[18], W. Wu[47], I. Yakushin[19], H. Yamamoto[17], Z. Yan[59], S. Yoshida[33], M. Zanolin[11], J. Zhang[51], L. Zhang[17], C. Zhao[59], N. Zotov[22], M. E. Zucker[20], H. zur Mühlen[16], J. Zweizig[17]
The LIGO Scientific Collaboration, http://www.ligo.org
April 30, 2009

ABSTRACT

We present the results of a LIGO search for short-duration gravitational waves (GWs) associated with the 2006 March 29 SGR 1900+14 storm. A new search method is used, "stacking" the GW data around the times of individual soft-gamma bursts in the storm to enhance sensitivity for models in which multiple bursts are accompanied by GW emission. We assume that variation in the time difference between burst electromagnetic emission and potential burst GW emission is small relative to the GW signal duration, and we time-align GW excess power time-frequency tilings containing individual burst triggers to their corresponding electromagnetic emissions. We use two GW emission models in our search: a fluence-weighted model and a flat (unweighted) model for the most electromagnetically energetic bursts. We find no evidence of GWs associated with either model. Model-dependent GW strain, isotropic GW emission energy $E_{\rm GW}$, and $\gamma \equiv E_{\rm GW}/E_{\rm EM}$ upper limits are estimated using a variety of assumed waveforms. The stacking method allows us to set the most stringent model-dependent limits on transient GW strain published to date. We find $E_{\rm GW}$ upper limit estimates (at a nominal distance of 10 kpc) of between 2×10^{45} erg and 6×10^{50} erg depending on waveform type. These limits are an order of magnitude lower than upper limits published previously for this storm and overlap with the range of electromagnetic energies emitted in SGR giant flares.

Subject headings: gravitational waves - soft gamma repeaters

1. INTRODUCTION

Soft gamma repeaters (SGRs) sporadically emit brief (~ 0.1 s) intense bursts of soft gamma-rays. Three of the five known SGRs have produced rare "giant flare" events with initial bright, short (~ 0.2 s) pulses with peak electromagnetic (EM) luminosities between 10^{44} and 10^{47} erg s^{-1}, placing them among the most EM luminous events in the Universe. According to the "magnetar" model SGRs are galactic neutron stars with extreme

[1] Albert-Einstein-Institut, Max-Planck-Institut für Gravitationsphysik, D-14476 Golm, Germany
[2] Albert-Einstein-Institut, Max-Planck-Institut für Gravitationsphysik, D-30167 Hannover, Germany
[3] Andrews University, Berrien Springs, MI 49104 USA
[4] Australian National University, Canberra, 0200, Australia
[5] California Institute of Technology, Pasadena, CA 91125, USA
[6] Caltech-CaRT, Pasadena, CA 91125, USA
[7] Cardiff University, Cardiff, CF24 3AA, United Kingdom
[8] Carleton College, Northfield, MN 55057, USA
[9] Charles Sturt University, Wagga Wagga, NSW 2678, Australia
[10] Columbia University, New York, NY 10027, USA
[11] Embry-Riddle Aeronautical University, Prescott, AZ 86301 USA
[12] Eötvös University, ELTE 1053 Budapest, Hungary
[13] Hobart and William Smith Colleges, Geneva, NY 14456, USA
[14] Institute of Applied Physics, Nizhny Novgorod, 603950, Russia
[15] Inter-University Centre for Astronomy and Astrophysics, Pune - 411007, India
[16] Leibniz Universität Hannover, D-30167 Hannover, Germany
[17] LIGO - California Institute of Technology, Pasadena, CA 91125, USA
[18] LIGO - Hanford Observatory, Richland, WA 99352, USA
[19] LIGO - Livingston Observatory, Livingston, LA 70754, USA
[20] LIGO - Massachusetts Institute of Technology, Cambridge, MA 02139, USA
[21] Louisiana State University, Baton Rouge, LA 70803, USA
[22] Louisiana Tech University, Ruston, LA 71272, USA
[23] Loyola University, New Orleans, LA 70118, USA
[24] Montana State University, Bozeman, MT 59717, USA
[25] Moscow State University, Moscow, 119992, Russia
[26] NASA/Goddard Space Flight Center, Greenbelt, MD 20771, USA
[27] National Astronomical Observatory of Japan, Tokyo 181-8588, Japan
[28] Northwestern University, Evanston, IL 60208, USA
[29] Rochester Institute of Technology, Rochester, NY 14623, USA
[30] Rutherford Appleton Laboratory, HSIC, Chilton, Didcot, Oxon OX11 0QX United Kingdom
[31] San Jose State University, San Jose, CA 95192, USA
[32] Sonoma State University, Rohnert Park, CA 94928, USA
[33] Southeastern Louisiana University, Hammond, LA 70402, USA
[34] Southern University and A&M College, Baton Rouge, LA 70813, USA
[35] Stanford University, Stanford, CA 94305, USA
[36] Syracuse University, Syracuse, NY 13244, USA
[37] The Pennsylvania State University, University Park, PA 16802, USA
[38] The University of Melbourne, Parkville VIC 3010, Australia
[39] The University of Mississippi, University, MS 38677, USA
[40] The University of Sheffield, Sheffield S10 2TN, United Kingdom
[41] The University of Texas at Austin, Austin, TX 78712, USA
[42] The University of Texas at Brownsville and Texas Southmost College, Brownsville, TX 78520, USA
[43] Trinity University, San Antonio, TX 78212, USA
[44] Universitat de les Illes Balears, E-07122 Palma de Mallorca, Spain
[45] University of Adelaide, Adelaide, SA 5005, Australia
[46] University of Birmingham, Birmingham, B15 2TT, United Kingdom
[47] University of Florida, Gainesville, FL 32611, USA
[48] University of Glasgow, Glasgow, G12 8QQ, United Kingdom
[49] University of Maryland, College Park, MD 20742 USA
[50] University of Massachusetts - Amherst, Amherst, MA 01003, USA
[51] University of Michigan, Ann Arbor, MI 48109, USA
[52] University of Minnesota, Minneapolis, MN 55455, USA
[53] University of Oregon, Eugene, OR 97403, USA
[54] University of Rochester, Rochester, NY 14627, USA
[55] University of Salerno, 84084 Fisciano (Salerno), Italy
[56] University of Sannio at Benevento, I-82100 Benevento, Italy
[57] University of Southampton, Southampton, SO17 1BJ, United Kingdom
[58] University of Strathclyde, Glasgow, G1 1XQ, United Kingdom
[58] University of Western Australia, Crawley, WA 6009, Australia
[60] University of Wisconsin-Milwaukee, Milwaukee, WI 53201, USA
[61] Washington State University, Pullman, WA 99164, USA

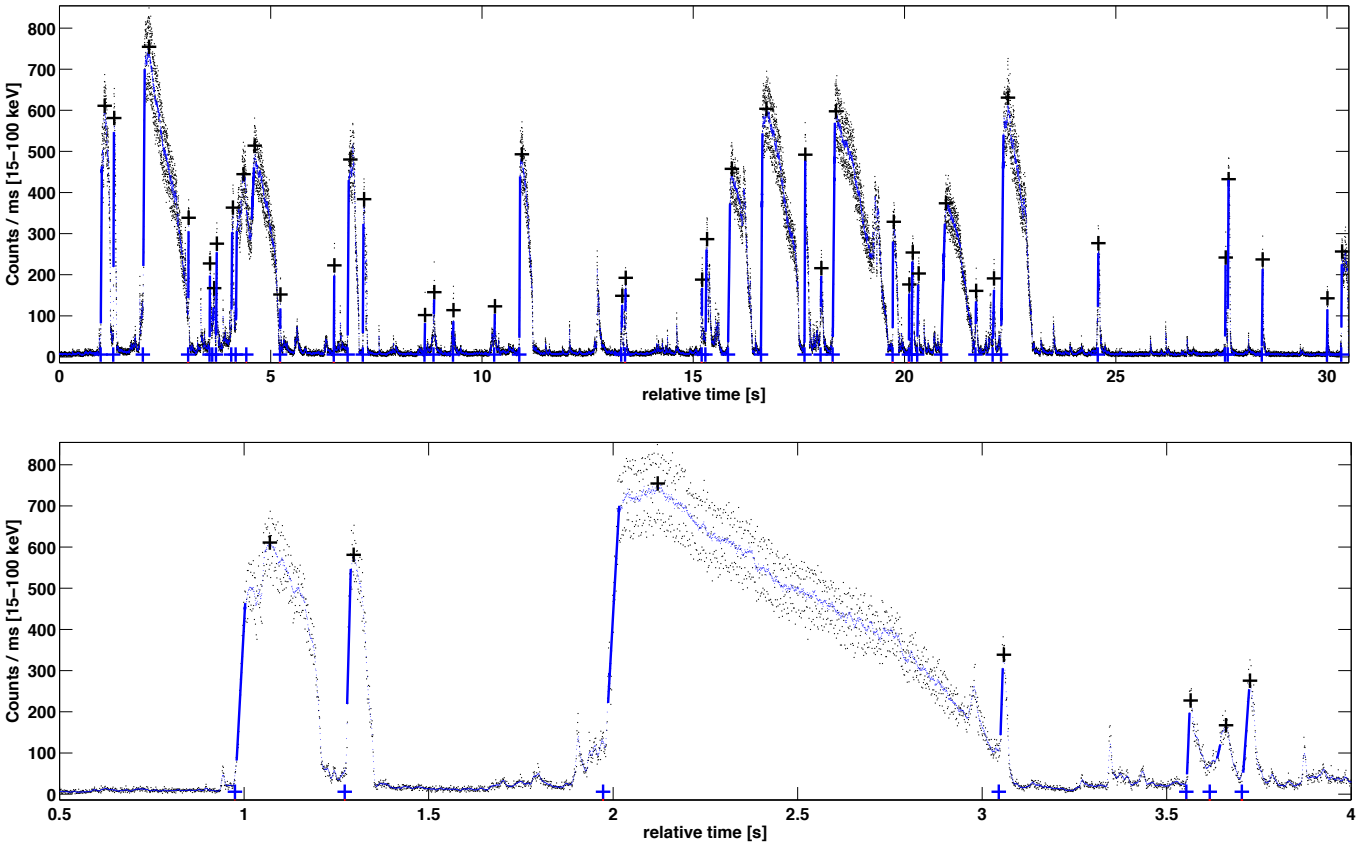

FIG. 1.— SGR 1900+14 storm light curve with 1 ms bins in the (15–100) keV band. Bottom plot shows a detail. Burst start times are estimated by fitting the steeply rising burst edges; EM fluences are estimated by integrating light curve area under each burst. A 30-bin running average is shown in addition to the raw light curve. Solid lines are linear fits to rising edges; the boundaries of rising edges were found by examining the first derivatives in the neighborhoods of the peak locations. Crosses mark burst peaks and intersections of the rising edge fits extrapolated to a linear fit of the noise floor measured in a quiescent period of data in the 50 s BAT sequence before the start of the storm. The one-sigma timing uncertainty averaged over all measurements is 2.9 ms. X-axis times are relative to 2006-03-29 02:53:09.9 UT at the Swift satellite.

magnetic fields $\sim 10^{15}$ G (Duncan & Thompson 1992). Bursts may result from the interaction of the star's magnetic field with its solid crust, leading to crustal deformations and occasional catastrophic cracking (Thompson & Duncan 1995; Schwartz et al. 2005; Horowitz & Kadau 2009) with subsequent excitation of nonradial neutron star f-modes (Andersson & Kokkotas 1998; de Freitas Pacheco 1998; Ioka 2001) and the emission of GWs (Owen 2005; Horvath 2005; de Freitas Pacheco 1998; Ioka 2001). For reviews, see Mereghetti (2008); Woods & Thompson (2004).

Occasionally SGRs produce many soft-gamma bursts in a brief period of time; such intense emissions are referred to as "storms." We present a search for short-duration GW signals ($\lesssim$0.3 s) associated with *multiple* bursts in the 2006 March 29 SGR 1900+14 storm (Israel et al. 2008) using data collected by the Laser Interferometer Gravitational Wave Observatory (LIGO) (Abbott et al. 2007). The storm light curve, obtained from the Burst Alert Telescope (BAT) aboard the Swift satellite (Barthelmy et al. 2005), is shown in Fig. 1. It consists of more than 40 bursts in ~30 s, including common SGR bursts and some intermediate flares with durations $>$ 0.5 s. The total fluence for the storm event was estimated by the Konus-Wind team to be $(1-2)\times10^{-4}$ erg cm^{-2} in the (20–200) keV range (Golenetskii et al. 2006), implying an isotropic EM energy $E_{\rm EM} = (1-2)\times10^{42}$ erg at a nominal distance to SGR 1900+14 of 10 kpc (source location and distance is discussed in Kaplan et al. (2002)). At the time of the storm both of the 4 km LIGO detectors (located at Hanford, WA and Livingston, LA) were taking science quality data.

We attempt to improve sensitivity to multiple weak GW burst signals associated with the storm's multiple EM bursts by adding together GW signal power over multiple bursts. In doing so we assume particular GW emission models, which we describe in the next section. Fig. 2 illustrates the stacking procedure using the four most energetic bursts in the storm.

2. METHODS

The analysis is performed by the Stack-a-flare pipeline (Kalmus et al. 2009), which extends the method used in a recent LIGO search for transient GW associated with individual SGR bursts (Abbott et al. 2008) and relies on an excess power detection statistic (Anderson et al. 2001). To "stack" N bursts in the storm, we first generate N excess power time-frequency tilings. These are 2-dimensional matrices in time and frequency generated from the two detectors' data streams. Each tiling element gives an excess power estimate in the GW detector data stream in a small period of time δt and a small range of frequency δf. The time range of each tiling is chosen to be centered on the time of one of the target EM bursts in the storm. We then align these N tilings

along the time dimension so that times of the target EM bursts coincide, and perform a weighted addition.

Stacking significantly improves sensitivity to GW emission under a given model. However, improving detection probability depends upon stacking according to GW emission models that correctly describe nature. The storm light curve motivated two stacking models: a flat-weighted model which includes the 11 most energetic EM bursts with unity weighting factors; and an EM-fluence-weighted model comprised of the 18 most energetic EM bursts. The $N = 11$ cutoff in the flat model is motivated by a clear separation in EM fluence of the 11 most energetic bursts in the storm. Including the 18 most energetic bursts in the fluence-weighted model accounts for 95% of the total EM fluence of the more than 40 bursts in the light curve. In the fluence-weighted model, time-frequency excess power tilings are weighted according to burst-integrated BAT counts before stacking. Further details are in Kalmus et al. (2009).

To obtain estimates of the times of EM bursts in the storm, we measure the intersections of the rapid rising edges of each burst with the light curve noise floor measured in a quiescent period of data in the 50 s BAT sequence before the start of the storm (Fig. 1). We correct these times for satellite-to-geocenter times-of-flight using the known SGR 1900+14 sky position and Swift ephemeris, which vary from (17.12–17.48) ms over the ∼30 s duration of the storm. The stack-a-flare analysis method is robust to relative timing errors smaller than GW signal durations (Kalmus et al. 2009). EM fluences are estimated by integrating detector counts under each burst in the light curve. We conservatively converted counts to fluences using the lower bound of the Konus-Wind total fluence range given above.

We divide the GW data into an on-source time region, in which GWs associated with the storm could be expected, and a background region, with statistically similar noise in which we do not expect a GW. This is done after applying category 1 and category 2 data quality cuts described in Abbott et al. (2009). The on-source region consists of 4 s of stacked data. Each 4 s region comprising the stack is centered on the time of one of the EM bursts included in the GW emission stacking model. Background regions consist of 1000 s of data on either side of the storm. On-source and background segments are analyzed and stacked identically, and the stacked time-frequency tilings are passed through a clustering algorithm resulting in lists of "analysis events." Background analysis events due to fluctuating detector noise are used to estimate the significance of on-source events; significant events, if any, are subject to vetoes (Abbott et al. 2009).

Using ±2 s regions around bursts in the storm accounts for uncertainties in the EM burst times and a possible systematic delay between GW and EM emission. Although GW emission in SGRs is expected to occur almost simultaneously with the EM burst (Ioka 2001), a common bias in trigger times shared by all bursts in the stacking set of $\lesssim$1 s can be handled with a ±2 s on-source region.

As in Abbott et al. (2008), this search targets neutron star fundamental mode ringdowns (RDs) predicted in Andersson & Kokkotas (1998); de Freitas Pacheco (1998); Ioka (2001); Andersson (2003) as well as short-duration GW signals of unknown waveform. RDs are targeted because f-modes are the most efficient GW emitters (Andersson & Kokkotas 1998). We assume that given a neutron star, f-mode frequencies and damping timescales would be similar from event to event, and that unknown signals would at least have similar central frequencies and durations from event to event.

As in Abbott et al. (2008), we thus focus on two distinct regions in the target signal time-frequency parameter space. The first region targets ∼100-400 ms duration signals in the (1–3) kHz band, which includes f-mode RD signals predicted in Benhar et al. (2004) for ten realistic neutron star equations of state. We choose a search band of (1–3) kHz for RD searches, with a 250 ms time window which was found to give optimal search sensitivity (Kalmus 2008). The second region targets ∼(5–200) ms duration signals in the (100–1000) Hz band. The target durations are set by prompt SGR burst timescales (5 ms to 200 ms) and the target frequencies are set by the detector's sensitive region. We search in two bands: (100–200) Hz (probing the region in which the detectors are most sensitive) and (100–1000) Hz (for full spectral coverage below the RD search band) using a 125 ms time window. In all, we search in three frequency bands and two GW emission models (flat and fluence-weighted). This amounts to a total of six 4 s-long stacked on-source regions.

We estimate loudest-event upper limits (Brady et al. 2004) on GW root-sum-squared strain $h_{\rm rss}$ incident at the detector. We can construct simulations of impinging GW with a given $h_{\rm rss}$. Following Abbott et al. (2005b)

$$h_{\rm rss}^2 = h_{\rm rss+}^2 + h_{\rm rss\times}^2, \tag{1}$$

where e.g.

$$h_{\rm rss+}^2 = \int_{-\infty}^{\infty} |h_+|^2 \, dt \tag{2}$$

and $h_{+,\times}(t)$ are the two GW polarizations. The relationship between the GW polarizations and the detector response $h(t)$ to an impinging GW from a polar angle and azimuth (θ, ϕ) and with polarization angle ψ is:

$$h(t) = F_+(\theta,\phi,\psi)h_+(t) + F_\times(\theta,\phi,\psi)h_\times(t) \tag{3}$$

where $F_+(\theta,\phi,\psi)$ and $F_\times(\theta,\phi,\psi)$ are the antenna functions for the source at (θ,ϕ) (Thorne 1987). At the time of the storm, the polarization-independent RMS antenna response $(F_+^2 + F_\times^2)^{1/2}$, which indicates the average sensitivity to a given sky location, was 0.39 for LIGO Hanford observatory and 0.46 for the LIGO Livingston observatory.

We can also set upper limits on the emitted isotropic GW emission energy $E_{\rm GW}$ at a source distance R associated with $h_+(t)$ and $h_\times(t)$ via (Shapiro & Teukolsky 1983)

$$E_{\rm GW} = 4\pi R^2 \frac{c^3}{16\pi G} \int_{-\infty}^{\infty} \left((\dot{h}_+)^2 + (\dot{h}_\times)^2 \right) dt. \tag{4}$$

The procedure for estimating loudest-event upper limits in the individual burst search is detailed in Kalmus (2008); Abbott et al. (2008). In brief, the upper limit is computed in a frequentist framework by injecting artificial signals into the background data and recovering them with the search pipeline (see for example Abbott

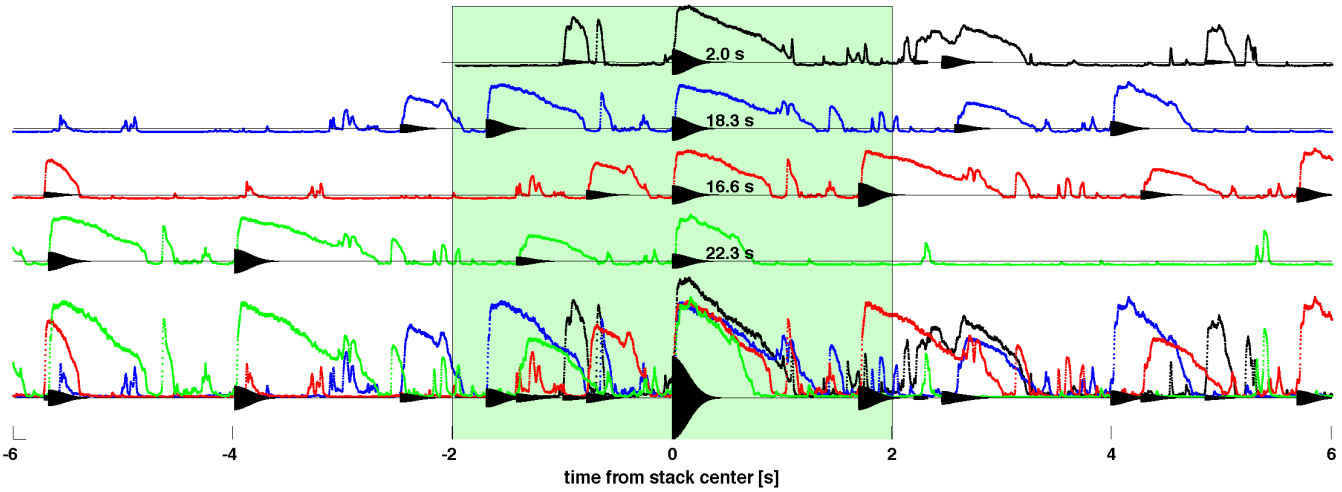

FIG. 2.— Individual EM bursts inform the stacking of GW data. This figure suggests the stacking procedure and explicitly shows search timescales. The top four plots are EM light curve time series around individual bursts beginning at 2.0 s, 16.6 s, 18.3 s, and 22.3 s in Fig. 1. Simulated GW ringdowns in the fluence-weighted model are superposed. The bottom plot shows the EM time series simultaneously, and the sum of the hypothetical GW signals. The on-source region of ±2 s is shaded. In the search, GW data corresponding to the EM time series are transformed to time-frequency power tilings before being added together and therefore there is no dependence on phase-coherence of GW signals in the analysis; this transformation is not illustrated.

et al. (2005a, 2008)). An analysis event is associated with each injection, and compared to the loudest on-source analysis event. The GW strain or isotropic energy at 90% detection efficiency is the strain or isotropic energy at which 90% of injections have associated events louder than the loudest on-source event.

We use the twelve waveform types described in Abbott et al. (2008) to establish detector sensitivity and thereby set upper limits: linearly and circularly polarized RDs with $\tau = 200$ ms and frequencies in the range (1–3) kHz; and band- and time-limited white noise bursts (WNBs) with durations of 11 ms and 100 ms and frequency bands matched to the two lower frequency search bands.

These waveforms are used to construct compound injections determined by the emission model. In the flat model, 11 GW bursts comprise a compound injection, each is identical, and our stated $h_{\rm rss}$ and $E_{\rm GW}$ are for one such GW burst in the compound injection. In the fluence-weighted model, 18 GW bursts comprise a compound injection, they are weighted (in amplitude) with the square root of integrated counts, and our stated $h_{\rm rss}$ and $E_{\rm GW}$ are for the loudest GW burst in the compound injection. A single polarization angle is chosen randomly for every compound injection. In assuming that the bursts emitted are identical up to an amplitude scale factor, we implicitly assume the star's GW emission mechanism and symmetry axis are constant over bursts in the storm.

3. RESULTS

We find no statistically significant GW signal associated with the SGR 1900+14 storm. The significance of on-source analysis events is inferred by noting the rate at which background analysis events of equal or greater loudness occur. We examined 4 s stacked on-source regions in the flat and fluence-weighted models in the three search bands. The most significant on-source analysis event from these six searches was from the flat model in the (100–1000) Hz band and had a corresponding background rate of 5.0×10^{-2} Hz (1 per 20 s) in that search.

Table 1 and Fig. 3 give model-dependent loudest-event upper limits at 90% detection efficiency computed for the GW signal associated with the single loudest EM burst. We give strain upper limits ($h_{\rm rss}^{90\%}$) and isotropic emission energy upper limits at a nominal SGR 1900+14 distance of 10 kpc ($E_{\rm GW}^{90\%}$). We also give upper limits $\gamma_{\rm UL} = E_{\rm GW}^{90\%}/E_{\rm EM}$, a source-distance-independent measure of the extent to which an energy upper limit probes the GW emission efficiency, calculated using a conservative estimate of 1.0×10^{-4} erg cm^{-2} for the total fluence of the storm to estimate fluences for individual peaks. In the fluence-weighted model, γ is the same for each individual burst. In the flat model we report the mean value of γ for the 11 bursts.

Superscripts in Table 1 give a systematic error and uncertainties at 90% confidence. (Similar estimates were made for the $E_{\rm GW}^{90\%}$ but are not shown in the table.) The first and second superscripts account for the systematic error and statistical uncertainty, respectively, in the detector calibrations. The third is the statistical uncertainty from using a finite number of trials (200) in the Monte Carlos, estimated with the bootstrap method using 200 ensembles (Efron 1979). The systematic error and the quadrature sum of the statistical uncertainties are added to the final sensitivity estimates. One-sigma burst timing uncertainties from fits of burst rising edges are accounted for in the Monte Carlo simulations. Estimating uncertainties is further described in Kalmus et al. (2009).

4. DISCUSSION

The stacked search described here extends the recent LIGO search for GW associated with the 2004 SGR 1806–20 giant flare and 190 lesser events from SGR 1806–20 and SGR 1900+14 (Abbott et al. 2008). That search was the first search sensitive to neutron star f-modes, and it set individual burst upper limits $E_{\rm GW}^{90\%}$ ranging

TABLE 1
Stack-a-flare SGR 1900+14 storm upper limits.

	N=11 Flat					N=18 Fluence-weighted				
Simulation type		$h_{\rm rss}^{90\%}[10^{-22}\ {\rm Hz}^{-\frac{1}{2}}]$		$E_{\rm GW}^{90\%}$ [erg]	$\gamma_{\rm UL}$		$h_{\rm rss}^{90\%}[10^{-22}\ {\rm Hz}^{-\frac{1}{2}}]$		$E_{\rm GW}^{90\%}$ [erg]	$\gamma_{\rm UL}$
WNB 11ms 100-200 Hz	1.3	$^{+0.0}\ ^{+0.17}\ ^{+0.0}$	$= 1.5$	1.9×10^{45}	3×10^4	2.1	$^{+0.0}\ ^{+0.27}\ ^{+0.094}$	$= 2.4$	5.0×10^{45}	3×10^4
WNB 100ms 100-200 Hz	1.5	$^{+0.0}\ ^{+0.19}\ ^{+0.0}$	$= 1.7$	2.4×10^{45}	4×10^4	2.3	$^{+0.0}\ ^{+0.30}\ ^{+0.098}$	$= 2.6$	6.0×10^{45}	3×10^4
WNB 11ms 100-1000 Hz	3.5	$^{+0.0}\ ^{+0.45}\ ^{+0.0}$	$= 3.9$	1.8×10^{47}	3×10^6	5.2	$^{+0.0}\ ^{+0.67}\ ^{+0.29}$	$= 5.9$	4.1×10^{47}	2×10^6
WNB 100ms 100-1000 Hz	3.8	$^{+0.0}\ ^{+0.50}\ ^{+0.0}$	$= 4.3$	2.0×10^{47}	3×10^6	5.6	$^{+0.0}\ ^{+0.73}\ ^{+0.29}$	$= 6.3$	4.5×10^{47}	2×10^6
RDC 200ms 1090 Hz	4.5	$^{+0.045}\ ^{+0.59}\ ^{+0.0}$	$= 5.2$	1.2×10^{48}	2×10^7	7.2	$^{+0.072}\ ^{+0.93}\ ^{+0.33}$	$= 8.2$	3.0×10^{48}	2×10^7
RDC 200ms 1590 Hz	6.4	$^{+0.19}\ ^{+0.84}\ ^{+0.0}$	$= 7.4$	5.1×10^{48}	8×10^7	11	$^{+0.33}\ ^{+1.4}\ ^{+0.44}$	$= 13$	1.5×10^{49}	8×10^7
RDC 200ms 2090 Hz	9.3	$^{+0.28}\ ^{+1.8}\ ^{+0.41}$	$= 11$	2.1×10^{49}	3×10^8	14	$^{+0.43}\ ^{+2.8}\ ^{+0.72}$	$= 18$	4.9×10^{49}	3×10^8
RDC 200ms 2590 Hz	11	$^{+0.34}\ ^{+2.2}\ ^{+0.32}$	$= 14$	4.6×10^{49}	8×10^8	17	$^{+0.50}\ ^{+3.3}\ ^{+1.0}$	$= 21$	1.0×10^{50}	5×10^8
RDL 200ms 1090 Hz	9.3	$^{+0.0}\ ^{+1.2}\ ^{+0.95}$	$= 11$	5.3×10^{48}	9×10^7	16	$^{+0.0}\ ^{+2.1}\ ^{+1.6}$	$= 18$	1.5×10^{49}	8×10^7
RDL 200ms 1590 Hz	14	$^{+0.42}\ ^{+1.8}\ ^{+1.1}$	$= 17$	2.6×10^{49}	4×10^8	19	$^{+0.58}\ ^{+2.5}\ ^{+1.9}$	$= 23$	5.1×10^{49}	3×10^8
RDL 200ms 2090 Hz	20	$^{+1.2}\ ^{+3.9}\ ^{+1.4}$	$= 25$	1.0×10^{50}	2×10^9	27	$^{+1.6}\ ^{+5.3}\ ^{+2.8}$	$= 34$	1.9×10^{50}	1×10^9
RDL 200ms 2590 Hz	25	$^{+1.8}\ ^{+5.0}\ ^{+3.0}$	$= 33$	2.6×10^{50}	4×10^9	39	$^{+2.7}\ ^{+7.7}\ ^{+2.5}$	$= 50$	6.2×10^{50}	3×10^9

from 3×10^{45} erg to 9×10^{52} erg (depending on waveform type and detector antenna factors and noise characteristics at the time of the burst), but did not detect any GWs. The best values of $\gamma_{\rm UL}$ in Abbott et al. (2008), for the giant flare, were in the range 5×10^1–6×10^6 depending on waveform type.

The upper limits obtained here are a factor of 12 more sensitive in energy than the SGR 1900+14 storm upper limits in Abbott et al. (2008), which analyzed the storm in a single ±20 s on-source region. Those previous limits already overlapped the range of EM energies seen in the loudest flares as well as the range of GW energies predicted by the most extreme models (Ioka 2001). The flat model gives isotropic energy upper limits on average a factor of 4 lower than a reference $N = 1$ (non-stacked) scenario (with a ±2 s on-source region) and a factor of 2 lower than the fluence-weighted model. However, our storm γ upper limits are still a few hundred times the SGR 1806–20 giant flare γ upper limits, due to the tremendous EM energy released by the giant flare. There is very little discussion of γ in the theory literature with which to compare.

The Advanced LIGO detectors promise an improvement in energy sensitivity of more than a factor of 100. Furthermore, on 2008 August 22, SGR 0501+4516 was discovered (Holland et al. 2008; Barthelmy et al. 2008; Palmer & Barthelmy 2008) and may be located only 1.5 kpc away (Gaensler & Chatterjee 2008; Leahy & Aschenbach 1995). SGR 0501+4516 searches will thus gain an additional 2 orders of magnitude in energy and γ upper limits compared to SGRs at 10 kpc. A stacking analysis of SGR 0501+4516 bursts with Advanced LIGO (a gain of 4 orders of magnitude in energy sensitivity) could therefore reach γ values below unity, even without another giant flare.

In the future we plan to carry out stacking searches on isolated SGR bursts, and eventually to perform searches using Advanced LIGO data. Our stacked upper limits depend on theoretical guidance as to what weightings and time delays are possible, and the significance of our results depends on predictions of the range of $E_{\rm GW}$ and γ; yet all of these things are scarce. We hope that our continued efforts to search for GW associated with SGR and Anomalous X-ray Pulsar bursts encourage further modeling of GW emission from these intriguing objects.

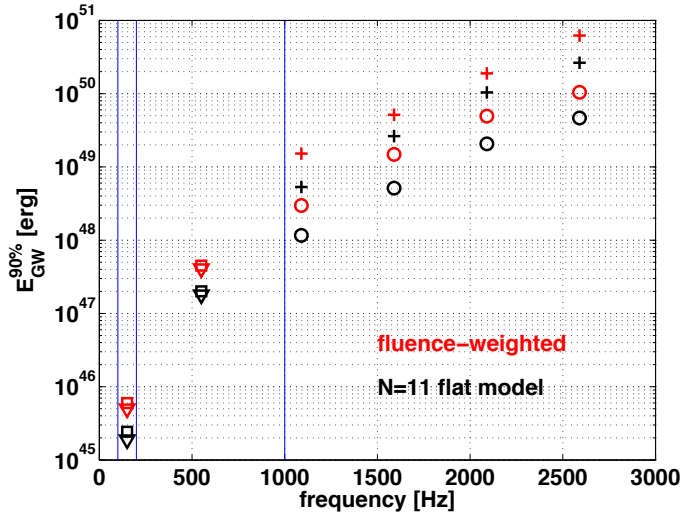

Fig. 3.— Stack-a-flare SGR 1900+14 storm isotropic energy upper limit estimates at 10 kpc, for flat and fluence-weighted emission models. We set upper limits at characteristic points in the signal parameter space in order to quantify the meaning of our non-detection result. Uncertainties have been folded in. Vertical lines indicate boundaries of the three distinct search frequency bands. Crosses and circles indicate linearly and circularly polarized RDs, respectively. Triangles and squares represent 11 ms and 100 ms band- and time-limited WNBs, respectively. Symbols are placed at the waveform central frequency. These results reflect the noise curves of the detectors.

The authors are grateful to the Swift team for the SGR 1900+14 storm data. The authors gratefully acknowledge the support of the United States National Science Foundation for the construction and operation of the LIGO Laboratory and the Science and Technology Facilities Council of the United Kingdom, the Max-Planck-Society, and the State of Niedersachsen/Germany for support of the construction and operation of the GEO600 detector. The authors also gratefully acknowledge the support of the research by these agencies and by the Australian Research Council, the Council of Scientific and Industrial Research of India, the Istituto Nazionale di Fisica Nucleare of Italy, the Spanish Ministerio de Educación y Ciencia, the Conselleria d'Economia Hisenda i Innovació of the Govern de les Illes Balears, the Royal Society, the Scottish Funding Council, the Scottish Universities Physics Alliance, The National Aeronautics and Space Administration, the Carnegie Trust, the Lever-

hulme Trust, the David and Lucile Packard Foundation, the Research Corporation, and the Alfred P. Sloan Foundation. This Letter is LIGO-P0900024.

REFERENCES

Abbot, B. et al. 2009, in preparation
—. 2005a, Phys. Rev. D, 72, 082001
—. 2005b, Phys. Rev. D, 72, 062001
—. 2007, ArXiv e-prints 0711.3041
—. 2008, Phys. Rev. Lett., 101, 211102
—. 2008, Phys. Rev. D, 77, 062004
Anderson, W. G., Brady, P. R., Creighton, J. D., & Flanagan, É. É. 2001, Phys. Rev. D, 63, 042003
Andersson, N. 2003, Class. Quant. Grav., 20, 105
Andersson, N. & Kokkotas, K. D. 1998, MNRAS, 299, 1059
Barthelmy, S. et al. 2005, Space Sci. Rev., 120, 143
—. 2008, GRB Coordinates Network, 8113
Benhar, O., Ferrari, V., & Gualtieri, L. 2004, Phys. Rev. D, 70, 124015
Brady, P. R., Creighton, J. D. E., & Wiseman, A. G. 2004, Class. Quant. Grav., 21, S1775
de Freitas Pacheco, J. A. 1998, A&A, 336, 397
Duncan, R. C. & Thompson, C. 1992, ApJ Lett., 392, L9
Efron, B. 1979, Ann. Statist., 7, 1
Gaensler, B. M. & Chatterjee, S. 2008, GRB Coordinates Network, 8149
Golenetskii, S. et al. 2006, GRB Coordinates Network, 4946
Holland, S. T. et al. 2008, GRB Coordinates Network, 8112
Horowitz, C. J. & Kadau, K. 2009, ArXiv e-prints 0904.1986
Horvath, J. E. 2005, Modern Physics Lett. A, 20, 2799
Ioka, K. 2001, MNRAS, 327, 639
Israel, G. L. et al. 2008, ApJ, 685, 1114
Kalmus, P. 2008, PhD thesis, Columbia University, ArXiv e-prints 0904.4394
Kalmus, P., Cannon, K. C., Márka, S., & Owen, B. J. 2009, ArXiv e-prints 0904.4906
Kaplan, D. L., Kulkarni, S. R., Frail, D. A., & van Kerkwijk, M. H. 2002, ApJ, 566, 378
Leahy, D. A. & Aschenbach, B. 1995, A&A, 293, 853
Mereghetti, S. 2008, A&A Rev., 15, 225
Owen, B. J. 2005, Phys. Rev. Lett., 95, 211101
Palmer, D. & Barthelmy, S. 2008, GRB Coordinates Network, 8115
Schwartz, S. J. et al. 2005, ApJ Lett., 627, L129
Shapiro, S. & Teukolsky, S. 1983, Black Holes, White Dwarfs, and Neutron Stars (New York: Wiley)
Thompson, C. & Duncan, R. C. 1995, MNRAS, 275, 255
Thorne, K. S. 1987, in 300 Years of Gravitation, ed. S. W. Hawking & W. Israel (Cambridge: Cambridge University Press), 417
Woods, P. M. & Thompson, C. 2004, in Compact Stellar X-Ray Sources, ed. W. G. H. Lewin & M. van der Klis (Cambridge: Cambridge Univ. Press)